Biochemical and Biophysical Research Communications 459 (2015) 547–552

Contents lists available at ScienceDirect

Biochemical and Biophysical Research Communications

journal homepage: www.elsevier.com/locate/ybbrc

Crystal structure and biochemical properties of *Re*H16_A1887, the 3-ketoacyl-CoA thiolase from *Ralstonia eutropha* H16

Jieun Kim, Kyung-Jin Kim*

School of Life Sciences, KNU Creative BioResearch Group, Kyungpook National University, Daehak-ro 80, Buk-ku, Daegu 702-701, Republic of Korea

ARTICLE INFO

Article history:
Received 13 February 2015
Available online 6 March 2015

Keywords:
Ralstonia eutropha
3-Ketoacyl-CoA thiolase
Structure
Polyhydroxyalkanoate

ABSTRACT

*Re*H16_A1887 from *Ralstonia eutropha* is an enzyme annotated as a 3-ketoacyl-CoA thiolase, and it catalyzes the fourth step of β-oxidation degradative pathways by converting 3-ketoacyl-CoA to acyl-CoA. We determined the crystal structures of *Re*H16_A1887 in the apo-form and in complex with its CoA substrate. *Re*H16_A1887 functions as a dimer, and the monomer of *Re*H16_A1887 comprises three subdomains (I, II, and III). The structural comparison between the apo-form and the CoA-bound form revealed that *Re*H16_A1887 undergoes a structural change in the lid-subdomain (subdomain III) upon the binding of the CoA substrate. The CoA molecule was stabilized by hydrogen bonding with positively charged residues such as Lys18, Arg210, and Arg217, and residues Thr213 and Gln151 aid its binding as well. At the active site of *Re*H16_A1887, highly conserved residues such as Cys91, His348, and Cys378 were located near the thiol-group of CoA, indicating that *Re*H16_A1887 might catalyze the thiolase reaction in a way similar to other thiolases. Moreover, in the vicinity of the covalent nucleophile Cys91, a hydrophobic hole that might serve as a binding site for the acyl-group of 3-ketoacyl-CoA was observed. The residues involved in enzyme catalysis and substrate-binding were further confirmed by site-directed mutagenesis experiments.

1. Introduction

Ralstonia eutropha H16 first attracted biotechnological interest nearly 50 years ago with the realization that its ability to produce and store large amounts of polyhydroxyalkanoate (PHA) that could be harnessed to make biodegradable plastics. The strain can store PHA up to 80% of its cell dry weight as a result of nutrient limitation [1]. Many groups have explored production of PHAs from renewable carbon sources such as plant oils. Plant oils are a suitable carbon source for this endeavor as 3-hydroxyacyl coenzyme A (3-hydroxyacyl-CoA) PHA precursors can be produced from intermediates in the fatty acid degradation pathway [2,3]. Plant oils consist of triacylglycerols (TAGs), in which three fatty acids are joined to a glycerol backbone. Recently, plant oils have been explored as a possible feedstock alternative to petroleum for chemical production [4]. These oils can also be used as sources of carbon for bioplastic production by bacteria such as *R. eutropha*. *R. eutropha* must therefore employ a fatty acid degradation pathway to consume oils and fatty acids.

Fatty acids are fundamental biomolecules that are abundant in all life forms. With their enormous variation in chain length and degree of saturation, they are essential for energy storage, form structural entities in biomembranes, and serve as signaling molecules. Fatty acids are broken down in a cyclic manner, two carbons at a time, to generate a range of products by the process known as β-oxidation [5]. The shortened fatty acyl-CoA can then be subjected to further rounds of β-oxidation or directed to other pathways. The fatty acid β-oxidation spiral involves four enzymes, acyl-CoA dehydrogenase (ACD), 2-enoyl-CoA hydratase (ECH), L-3-hydroxyacyl-CoA dehydrogenase (HACD) and 3-ketoacyl-CoA thiolase (KACT) [6]. Among these enzymes, KACT catalyzes the degradative cleavage of a β-ketoacyl-CoA to acyl-CoA and a two-carbon shortened acyl-CoA [7,8].

There are two distinct forms of 3-ketoacyl-CoA thiolases. Type I is the 3-ketoacyl-CoA thiolase (EC 2.3.1.16), a catabolic enzyme performing the reverse Claisen condensation reaction involved in such as the β-oxidation cycle. Type II is the acetoacetyl-CoA thiolase (ACAT; EC 2.3.1.9), which is involved in the anabolic mevalonate pathway performing Claisen condensation. *R. eutropha* possesses both type I and II thiolases. The fatty acid β-oxidation pathway in

* Corresponding author. Structural and Molecular Biology Laboratory, School of Life Sciences, Kyungpook National University, Daehak-ro 80, Buk-ku, Daegu 702-701, Republic of Korea. Fax: +82 53 955 5522.
E-mail address: kkim@knu.ac.kr (K.-J. Kim).

http://dx.doi.org/10.1016/j.bbrc.2015.02.148
0006-291X/

R. eutropha is uncharacterized in the literature. Most studies of microbial fatty acid β-oxidation have been conducted in *Escherichia coli* and *Bacillus subtilis* [9,10], although some information is available regarding fatty acid degradation in *Pseudomonas* species [11,12]. A search of the *R. eutropha* H16 genome reveals many potential β-oxidation pathway gene homologs [13]. For example, 50 genes in the *R. eutropha* H16 genome are annotated as enoyl-CoA hydratases and 46 genes are annotated as acyl-CoA dehydrogenases. However, it is not known which of these homologs actually play a role in fatty acid breakdown.

In this study, we aimed to determine the crystal structure of *Ralstonia eutropha* 3-ketoacyl-CoA thiolase A1887 (*Re*H16_A1887), an enzyme that catalyzes the fourth step of β-oxidation degradative pathways and converts 3-ketoacyl-CoA to acyl-CoA. Biochemical and mutagenesis experiments were also performed.

2. Materials and methods

2.1. Preparation of H16_A1887

Cloning, expression, purification, and crystallization of *Re*H16_A1887 will be described elsewhere (Kim et al., in preparation). Briefly, the *Re*H16_A1887 coding gene (Met1-Leu392, M.W. 41.5 kDa) was amplified by polymerase chain reaction using *R. eutropha* chromosomal DNA as a template. The PCR product was then subcloned into pET30a (Invitrogen), and the resulting expression vector pET30a: *Re*H16_A1887 was transformed into an *E. coli* BL21(DE3)-T1^{R} strain, which was grown in 1 L of LB medium containing kanamycin (50 mg/ml) at 37 °C. After induction via the addition of 1.0 mM IPTG, the culture medium was further maintained for 20 h at 18 °C. The culture was harvested by centrifugation at 4000 g at 4 °C. The cell pellet was resuspended in ice-cold buffer A (40 mM Tris–HCl at pH 8.0 and 5 mM β-mercaptoethanol) and then disrupted by ultrasonication. The cell debris was removed by centrifugation at 13,500 g for 25 m, and lysate was bound to an Ni-NTA agarose (QIAGEN). After washing with buffer A containing 20 mM imidazole, the bound proteins were eluted with 300 mM imidazole in buffer A. Finally, the trace amount of contamination was removed by applying Sephacryl S-300 HR prep grade (320 ml, GE Healthcare) size exclusion chromatography equilibrated with buffer A containing 5 mM β-mercaptoethanol (BME). All purification experiments were performed at 4 °C. The degree of protein purification was confirmed by SDS-PAGE. The purified protein showed ~95% purity on SDS-PAGE, was concentrated to 25 mg/ml in 40 mM Tris–HCl, pH 8.0, 5 mM BME.

2.2. Crystallization, data collection, and structure determination of ReH16_A1887

Crystallization of the purified protein was initially performed with commercially available sparse-matrix screens from RIGAKU and Molecular Dimensions using the hanging-drop vapor-diffusion method at 295 K. Each experiment consisted of mixing 1.2 μl protein solution (25 mg/ml in 40 mM Tris–HCl, pH 8.0) with 1.2 μl reservoir solution and then equilibrating it against 0.5 ml of the reservoir solution. *Re*H16_A1887 crystals were observed from several crystallization screening conditions. After several steps that improved the crystallization process using the hanging-drop vapor-diffusion method, crystals of the best quality appeared at 20 °C in 7 days and reached their maximal dimensions of approximately 0.2 × 0.2 × 0.5 mm using reservoir solution containing 17% PEG 8 K, 0.1 M HEPES, pH7.0.

The crystals were transferred to cryoprotectant solution containing 20% PEG 8 K, 0.1 M HEPES pH 7.0 and 30% (v/v) glycerol, fished out with a loop larger than the crystals and flash-frozen by immersion in liquid nitrogen at 100 K. The data were collected to a resolution of 1.4 Å at 7A beamline of the Pohang Accelerator Laboratory (PAL, Pohang, Korea) using a Quantum 270 CCD detector (ADSC, USA). The data were then indexed, integrated, and scaled using the HKL2000 suite [14]. Crystals of an apo-form belonged to space group $p4_32_12$, with unit cell parameters of $a = b = 129.52$ Å, $c = 114.13$ Å, $\alpha = \beta = \gamma = 90$. Assuming 2 molecules of *Re*H16_A1887 per asymmetric unit, the crystal volume per unit of protein mass was 2.99 Å^3 Da^{-1} [15], which corresponds to a solvent content of approximately 58.9%. *Re*H16_A1887 crystals in complex with CoA were crystallized with the same crystallization condition supplemented with 20 mM of CoA. Crystals in complex with CoA belonged to space group $p3_121$, with unit cell parameters of $a = b = 141.43$ Å, $c = 52.979$ Å, $\alpha = \beta = 90$ and $\gamma = 120$. Assuming 1 molecule of *Re*H16_A1887 per asymmetric unit, the crystal volume per unit of protein mass was 2.88 Å^3 Da^{-1} [15], which corresponds to a solvent content of approximately 57.36%.

The structure was determined by molecular replacement method with the CCP4 version of MOLREP using the structure of a thiolase from *Mycobacterium tuberculosis* (*Mt*FadA5, PDB code 4UBU) [16] as a search model. Model building was performed manually using the program WinCoot [17] and the refinement was performed with CCP4 refmac5 [18] and CNS [19]. The structures of *Re*H16_A1887 in complex with CoA were solved by molecular replacement method using the crystal structure of the apo-form of *Re*H16_A1887. Model building and structure refinement of the CoA-bound form were performed similarly to the apo-form of *Re*H16_A1887. The data statistics are summarized in Table 1. The refined *Re*H16_A1887 models will be deposited.

2.3. Activity measurement and site-directed mutagenesis

Site-specific mutations were created with the QuikChange kit (Stratagene), and sequencing was performed to confirm correct

Table 1
Data collection and refinement statistics.

	Apo	CoA-bound
Data collection		
Space group	$P4_32_12$	$P3_121$
Cell dimensions		
a, *b*, *c* (Å)	129.52,129.52, 114.13	141.43,141.43, 52.979
α, β, γ (°)	90.00, 90.00, 90.00	90.00, 90.00, 120.00
Resolution (Å)	50.0–1.4 (1.42–1.4)[a]	50.0–1.5 (1.53–1.5)
R_{sym} or R_{merge}	6.9 (30.9)	10.7 (34.0)
$I/\sigma(I)$	38.00 (3.78)	30.0 (4.8)
Completeness (%)	95.7 (87.2)	97.3 (93.2)
Redundancy	6.7 (4.2)	6.9 (3.9)
Refinement		
Resolution (Å)	50.0–1.4	50.0–1.5
No. reflections	172,263	89,331
R_{work}/R_{free}	15.6/18.1	15.20/17.61
No. atoms	6786	3396
Protein	5812	2906
Ligand/ion	–	48
Water	974	442
B-factors	17.531	12.564
Protein	15.869	11.041
Ligand/ion	–	15.206
Water	36.090	31.680
R.m.s. deviations		
Bond lengths (Å)	0.0291	0.0295
Bond angles (°)	2.6252	2.4719

AU: Equations defining various *R*-values are standard and hence are no longer defined in the footnotes.
AU: Ramachandran statistics should be in Methods section at the end of Refinement subsection.
AU: Wavelength of data collection, temperature and beamline should all be in Methods section.
[a] Number of xtals for each structure should be noted in footnote. Values in parentheses are for highest-resolution shell.

incorporation of the mutations. The activity measurement assays were performed with 1 ml total volume of reaction mixture, and all experiments were performed at 30 °C. The reaction mixture contained 0.1 M Tris–HCl, pH 8.3, 25 mM $MgCl_2$, 3-ketoacyl-CoA, 100 μM CoA, and 410 μM of *Re*H16_A1887 wild-type or mutant protein. After pre-incubation, the reaction was initiated by the addition of enzyme. The decrease in 3-ketoacyl-CoA was then measured at 303 nm using an extinction coefficient of $8.3 \times 10^3\ M^{-1}\ cm^{-1}$ [16,20].

3. Results and discussion

3.1. Overall structure of ReH16_A1887

To elucidate the enzymatic properties of the *Re*H16_A1887 protein, we determined the crystal structure of *Re*H16_A1887 at 1.4 Å. The asymmetric unit contains two *Re*H16_A1887 molecules, which corresponded to one biologically active dimer (Fig. 1). The size exclusion chromatography results also confirmed that *Re*H16_A1887 exists as a dimer (data not shown). A search using the Dali server revealed that the structure of *Re*H16_A1887 was homologous to that of FadA5, a thiolase from *M. tuberculosis* (*Mt*FadA5) [16]. The degradative thiolase class can form dimers or tetramers (the latter are built by dimers of dimers), but biosynthetic thiolases are reported to solely form tetramers [21,22]. *Re*H16_A1887 exists as a dimer both in the crystal and in solution (Fig. 1B). The N-terminal domain consisting of β -sheets (β1–β5) is involved in dimerization via hydrophobic interactions between β3 from each polypeptide. The interaction between α3 and α5 from the other chain also mediates the dimerization through hydrophobic interactions with residues such as Glu30, Leu74, Val71, Ile192, Ser139, Met140, Arg143 and Tyr 144.

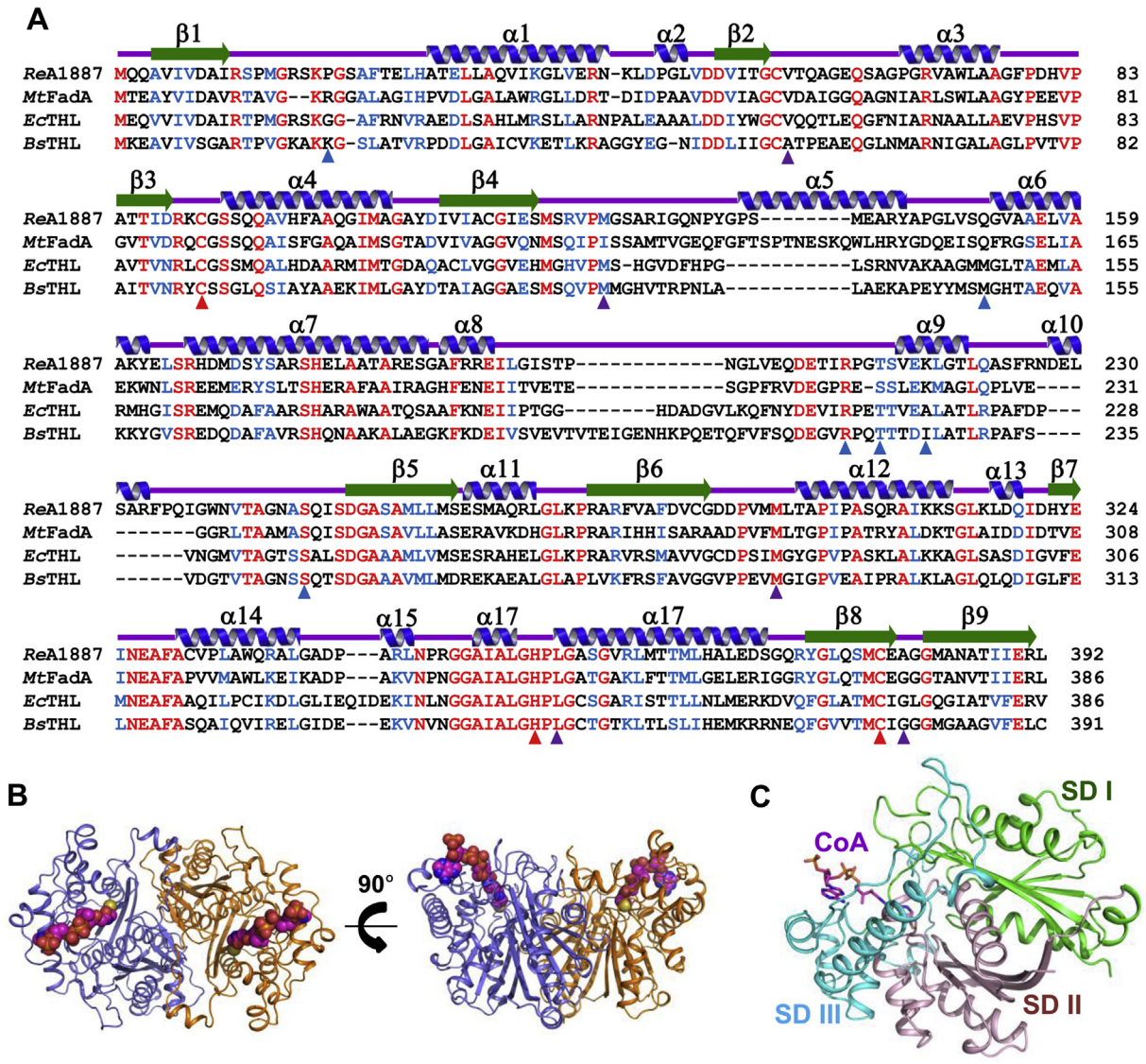

Fig. 1. Overall shape of *Re*H16_A1887. (A) Amino acid sequence alignment. Secondary structure elements are shown based on the *Re*H16_A1887 structure. Identical and highly conserved residues are presented in red and blue colored characters, respectively. Residues involved in the enzyme catalysis and CoA binding are marked with red and light-blue colors, respectively, and those constituting the acyl-group binding are with purple color. *Mt*FadA, *Ec*THL, *Bs*THL are abbreviations of thiolases from *Mycobacterium tuberculosis*, *Escherichia coli*, and *Bacillus subtillus*, respectively. (B) Dimeric structure of *Re*H16_A1887. A *Re*H16_A1887 dimer was shown as a cartoon model. Each monomer was distinguished with orange and light-blue colors. The bound CoA was shown as a sphere model with magentas color. The right side figure is 180° rotated vertically from the left side figure. (C) Monomeric structure of *Re*H16_A1887. Monomeric structure of *Re*H16_A1887 was shown as a cartoon diagram. The subdomain I, II, and III were distinguished with green, salmon, and cyan colors, respectively, and labeled as SD I, SD II, and SD III, respectively. The bound CoA was shown as a stick model with magentas color. (For interpretation of the references to colour in this figure legend, the reader is referred to the web version of this article.)

The monomeric *Re*H16_A1887 structure exhibits three-domain architecture (Fig. 1C). In this three subdomain model, residues M1-R123 and A246-L267 of *Re*H16_A1887 form subdomain I (N-terminal subdomain), residues G268–L392 form subdomain II (C-terminal subdomain), and residues V124–N245 form subdomain III (lid subdomain). Subdomains I and III are structurally and functionally related. These two subdomains are mainly characterized by a central β sheet (β1, β3, β3, β4 and β5 in subdomain I and β6–β9 in subdomain II) that is surrounded by four larger α helices (α1, α4, α12 and α17). The two subdomains harbor the active site residues of *Re*H16_A1887: Cys91 located next to β3 in subdomain I, and His348 (between helices α16 and α17) and Cys378 (at the end of β8) in subdomain II. The subdomain I/II architecture provides a stable and rather inflexible platform for the active site, whereas subdomain III sits on top of the two other domains and occludes the active site residues from the solvent. The lid-subdomain comprises an extended structure consisting of two helices, α6–α7, and four shorter helices, α5–α10. Positively charged residues are located along the cleft between subdomains I, II, and III, and some of these mediate the binding of the CoA substrate, which will be described later.

3.2. Lid subdomain movement upon the binding of substrate

In order to examine the substrate-binding mode, we determined the crystal structure of *Re*H16_A1887 in complex with the CoA substrate at a 1.5 Å resolution. The CoA substrate is positioned within the deep cleft between subdomains I, II, and III. The adenosine nucleotide moiety is exposed at the surface, whereas the thiol group is located in the vicinity of the catalytic site for the degradation reaction. Interestingly, the lid-subdomain undergoes a structural change of about 2.0 Å upon the binding of the CoA substrate (Fig. 2A). Especially, the Arg210 residue moved about 5.28 Å to constitute space for the binding of the adenosine ring. Moreover, the Lys217 residue located in α9 of the lid-subdomain moved about 5.48 Å, and the Leu221, Ser224, and Gln151 residues

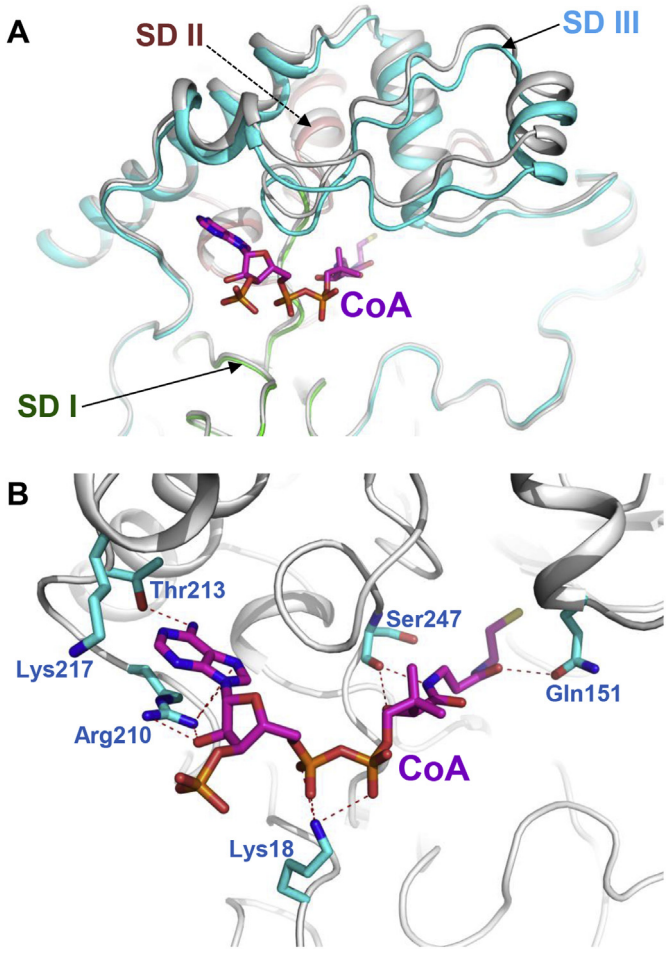

Fig. 2. CoA binding mode of *Re*H16_A1887. (A) Structural change of *Re*H16_A1887 upon the binding of CoA. The apo-form and CoA-bound form of *Re*H16_A1887 were superposed. The subdomain I (SD I), subdomain II (SD II), and subdomain III (SD III) of the CoA-bound form of *Re*H16_A1887 were distinguished with green, salmon, and cyan colors, respectively. The apo-form of *Re*H16_A1887 was drawn with gray color. The bound CoA was shown as a stick model with magentas color. (B) CoA-binding mode of *Re*H16_A1887. The CoA-bound form of *Re*H16_A1887 was drawn as a cartoon diagram with gray color. Residues involved in the binding of CoA were presented as stick model with cyan color, and labeled appropriately. The bound CoA was shown as a stick model with magentas color. (For interpretation of the references to colour in this figure legend, the reader is referred to the web version of this article.)

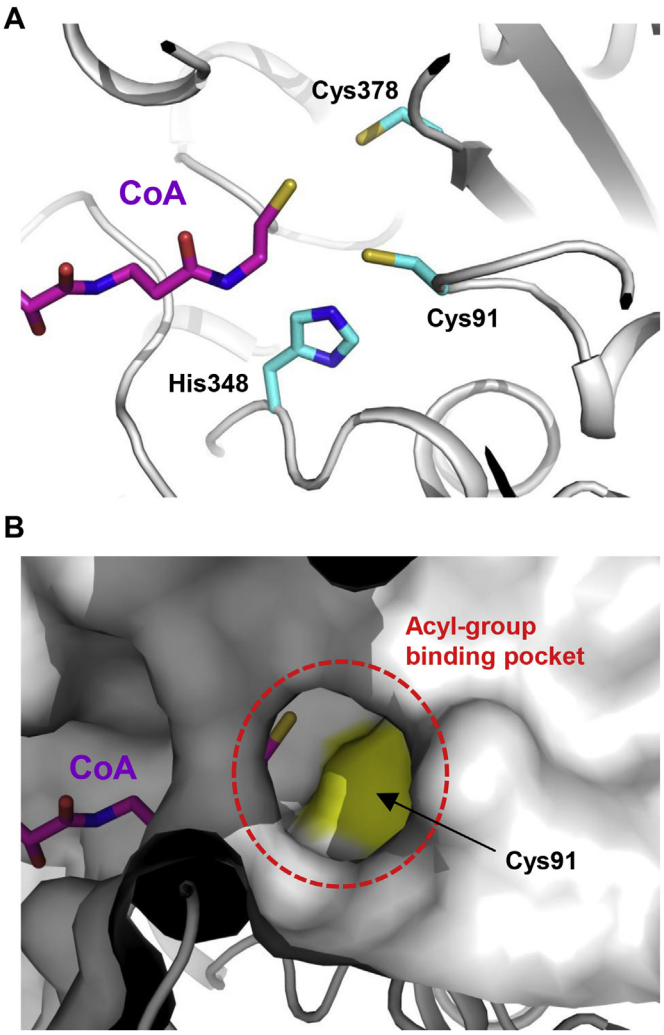

Fig. 3. Active site of *Re*H16_A1887. (A) Active site of *Re*H16_A1887. CoA-bound form of *Re*H16_A1887 was presented as a cartoon diagram with gray color. The catalytic residues were shown as stick model with cyan color, and labeled appropriately. The bound CoA was shown as a stick model with magentas color. (B) Acyl-CoA binding pocket. CoA-bound form of *Re*H16_A1887 was presented as a surface model with gray color. The position of the covalent neucleophile Cys91 was distinguished with yellow color and labeled. The acyl-CoA binding pocket was indicated with a red-colored dotted circle. The bound CoA was shown as a stick model with magentas color. (For interpretation of the references to colour in this figure legend, the reader is referred to the web version of this article.)

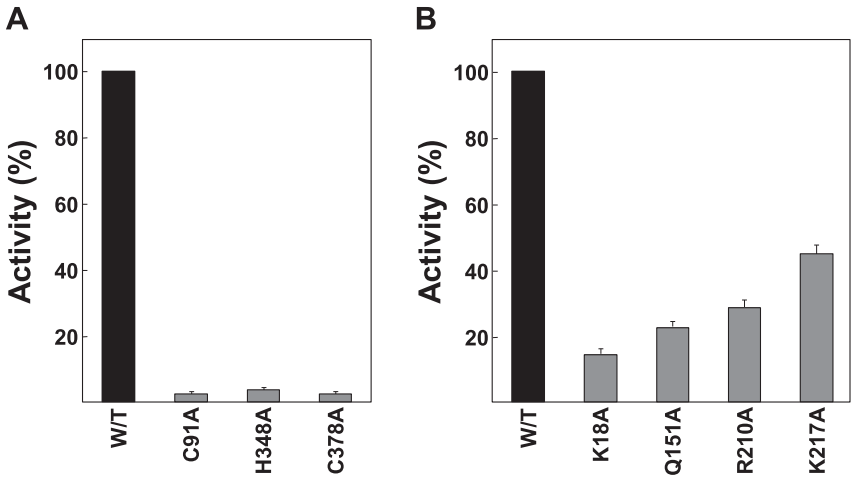

Fig. 4. Site-directed mutagenesis experiments. (A) (B) Site-directed mutagenesis for residues involved in the enzyme catalysis (A) and CoA binding (B). Residues involved in the enzyme catalysis and CoA-binding were replaced with alanine residues. The degradative thiolase activities of the recombinant mutant proteins were measured, and compared with that of the *Re*H16_A1887 wild-type. All experiments were performed in triplicate.

moved about 2.0 Å toward the bound CoA. The adenosine diphosphate moiety of CoA is stabilized by hydrogen bonding with positively charged residues such as Lys18, Arg210, and Lys217 (Fig. 2B). The pantothenic moiety of the substrate appears to be stabilized mainly by the side chain of Gln151, Met126, and Ser224 via hydrogen bonds, as well as via hydrogen bonds to the main chain of the Ile249 residue (Fig. 2B). The thiol group of CoA is located at its binding pocket and positioned near the conserved catalytic residues Cys91, His348, and Cys378, which correspond to the Cys93, His347, and Cys377 residues of *Mt*FadA5.

3.3. Enzyme catalysis of ReH16_A1887

Subdomains I and II harbor the active site residues of *Re*H16_A1887: Cys91 located between helices β3 and α4 in subdomain I, and His348 (between helices α16 and α17) and Cys378 (at the end of β8) in subdomain II (Fig. 3A). The positioning of Cys91 after β3 and right before α4 is likely to lower the pKa of this important nucleophile through its orientation with respect to the dipole moment of the helix. The first step of catalysis is conducted by Cys91 and His348; Cys91 functions as a covalent nucleophile, and His348 aids deprotonation of Cys91. Cys378 functions as a nucleophile in the second step of catalysis. In the vicinity of the covalent nucleophile Cys91, a hydrophobic hole is constituted by hydrophobic residues such as Val58, Met126, Met288, Leu350, and Ala380. This hole might provide space for the binding of the acyl-group that is covalently bound to thiol-group of Cys91 at the first step of the enzyme reaction (Fig. 3B). Because this hole is exposed to the solvent region, we suspect that *Re*H16_A1887 can utilize 3-ketoacyl-CoA with various lengths of carbon atoms as substrates. In fact, residues located in this region are variable throughout different organisms, indicating that the region might provide substrate specificity for 3-ketoacyl-group.

3.4. Site-directed mutagenesis studies

In order to confirm the residues involved in the enzyme catalysis and substrate binding mode of *Re*H16_A1887, we performed site-directed mutagenesis experiments based on structural observations of the protein, and compared the enzymatic activity of the mutants with that of the wild-type protein. To confirm residues involved in the enzyme catalysis, residues Cys91, His348, and Cys378 were mutated to alanine. As expected, the three mutants (C91A, H348A, and C378A) showed almost complete loss of activity (Fig. 4A). These results indicate that *Re*H16_A1887 uses these three residues for enzyme catalysis, and the enzyme uses enzyme reaction mechanism similar to other degradative thiolases. To confirm residues involved in the substrate stabilization, residues Lys18, Gln151, Arg210, and Lys217 were mutated to alanine. All mutants (K18A, Q151A, R210A, and K217A) showed reduced thiolase activity (Fig. 4B). Interestingly, the K217A mutant showed over 40% activity compared with the wild-type, which can be explained by the fact that Lys217 is not conserved across other organisms, and hydrogen bond formation between Lys217 and CoA is not obvious in our current structure.

Acknowledgments

This work was supported by the National Research Foundation of Korea (NRF) Grant funded by the Korean Government (MEST) (2014R1A2A2A01005752 and NRF-2014M1A2A2033626) and by the Advanced Biomass R&D Center (ABC) of Global Frontier Project funded by the MEST (2012M3A6A2053895).

Transparency document

Transparency document related to this article can be found online at http://dx.doi.org/10.1016/j.bbrc.2015.02.148.

References

[1] O.P. Peoples, A.J. Sinskey, Poly-beta-hydroxybutyrate (PHB) biosynthesis in *Alcaligenes eutrophus* H16. Identification and characterization of the PHB polymerase gene (phbC), J. Biol. Chem. 264 (1989) 15298–15303.
[2] R.G. Lageveen, G.W. Huisman, H. Preusting, P. Ketelaar, G. Eggink, B. Witholt, Formation of polyesters by *Pseudomonas oleovorans*: effect of substrates on formation and composition of poly-(R)-3-hydroxyalkanoates and poly-(R)-3-hydroxyalkenoates, Appl. Environ. Microbiol. 54 (1988) 2924–2932.
[3] M.T. Vo, K.W. Lee, Y.M. Jung, Y.H. Lee, Comparative effect of overexpressed phaJ and fabG genes supplementing (R)-3-hydroxyalkanoate monomer units on biosynthesis of mcl-polyhydroxyalkanoate in *Pseudomonas putida* KCTC1639, J. Biosci. Bioeng. 106 (2008) 95–98.
[4] A.S. Carlsson, Plant oils as feedstock alternatives to petroleum - a short survey of potential oil crop platforms, Biochimie 91 (2009) 665–670.
[5] D. Knoop, Industrial Conciliation and Arbitration, P. S. King, London, 1905.
[6] J.J. Kim, K.P. Battaile, Burning fat: the structural basis of fatty acid beta-oxidation, Curr. Opin. Struct. Biol. 12 (2002) 721–728.
[7] H.F. Gilbert, Proton transfer from acetyl-coenzyme A catalyzed by thiolase I from porcine heart, Biochemistry 20 (1981) 5643–5649.

[8] H.F. Gilbert, B.J. Lennox, C.D. Mossman, W.C. Carle, The relation of acyl transfer to the overall reaction of thiolase I from porcine heart, J. Biol. Chem. 256 (1981) 7371–7377.
[9] Y. Fujita, H. Matsuoka, K. Hirooka, Regulation of fatty acid metabolism in bacteria, Mol. Microbiol. 66 (2007) 829–839.
[10] H. Matsuoka, K. Hirooka, Y. Fujita, Organization and function of the YsiA regulon of *Bacillus subtilis* involved in fatty acid degradation, J. Biol. Chem. 282 (2007) 5180–5194.
[11] A. Chung, Q. Liu, S.P. Ouyang, Q. Wu, G.Q. Chen, Microbial production of 3-hydroxydodecanoic acid by pha operon and fadBA knockout mutant of *Pseudomonas putida* KT2442 harboring tesB gene, Appl. Microbiol. Biotechnol. 83 (2009) 513–519.
[12] S. Fiedler, A. Steinbuchel, B.H. Rehm, The role of the fatty acid beta-oxidation multienzyme complex from *Pseudomonas oleovorans* in polyhydroxyalkanoate biosynthesis: molecular characterization of the fadBA operon from *P. oleovorans* and of the enoyl-CoA hydratase genes phaJ from *P. oleovorans* and *Pseudomonas putida*, Arch. Microbiol. 178 (2002) 149–160.
[13] A. Pohlmann, W.F. Fricke, F. Reinecke, B. Kusian, H. Liesegang, R. Cramm, T. Eitinger, C. Ewering, M. Potter, E. Schwartz, A. Strittmatter, I. Voss, G. Gottschalk, A. Steinbuchel, B. Friedrich, B. Bowien, Genome sequence of the bioplastic-producing "Knallgas" bacterium *Ralstonia eutropha* H16, Nat. Biotechnol. 24 (2006) 1257–1262.
[14] Z. Otwinowski, W. Minor, Processing of X-ray diffraction data collected in oscillation mode, Macromol. Crystallogr. Pt A 276 (1997) 307–326.
[15] B.W. Matthews, Solvent content of protein crystals, J. Mol. Biol. 33 (1968) 491–497.
[16] J.J. Barycki, L.K. O'Brien, J.M. Bratt, R. Zhang, R. Sanishvili, A.W. Strauss, L.J. Banaszak, Biochemical characterization and crystal structure determination of human heart short chain L-3-hydroxyacyl-CoA dehydrogenase provide insights into catalytic mechanism, Biochemistry 38 (1999) 5786–5798.
[17] P. Emsley, K. Cowtan, Coot: model-building tools for molecular graphics, Acta Crystallogr. D Biol. Crystallogr. 60 (2004) 2126–2132.
[18] G.N. Murshudov, A.A. Vagin, E.J. Dodson, Refinement of macromolecular structures by the maximum-likelihood method, Acta Crystallogr. D. Biol. Crystallogr. 53 (1997) 240–255.
[19] A.T. Brunger, P.D. Adams, G.M. Clore, W.L. DeLano, P. Gros, R.W. Grosse-Kunstleve, J.S. Jiang, J. Kuszewski, M. Nilges, N.S. Pannu, R.J. Read, L.M. Rice, T. Simonson, G.L. Warren, Crystallography & NMR system: a new software suite for macromolecular structure determination, Acta Crystallogr. D Biol. Crystallogr. 54 (1998) 905–921.
[20] R.C. Taylor, A.K. Brown, A. Singh, A. Bhatt, G.S. Besra, Characterization of a beta-hydroxybutyryl-CoA dehydrogenase from *Mycobacterium tuberculosis*, Microbiology 156 (2010) 1975–1982.
[21] P. Kursula, J. Ojala, A.M. Lambeir, R.K. Wierenga, The catalytic cycle of biosynthetic thiolase: a conformational journey of an acetyl group through four binding modes and two oxyanion holes, Biochemistry 41 (2002) 15543–15556.
[22] Y. Modis, R.K. Wierenga, A biosynthetic thiolase in complex with a reaction intermediate: the crystal structure provides new insights into the catalytic mechanism, Structure 7 (1999) 1279–1290.